JOURNAL OF GEOPHYSICAL RESEARCH, VOL. 104, NO. D3, PAGES 3483–3500, FEBRUARY 20, 1999

Is aerosol production within the remote marine boundary layer sufficient to maintain observed concentrations?

Kevin P. Capaldo

Department of Chemical Engineering, Carnegie Mellon University, Pittsburgh, Pennsylvania

Prasad Kasibhatla

Nicholas School of the Environment, Duke University, Durham, North Carolina

Spyros N. Pandis

Department of Chemical Engineering and Department of Engineering and Public Policy, Carnegie Mellon University, Pittsburgh, Pennsylvania

Abstract. To evaluate the impact of aerosols on climate we must consider the aerosol dynamics of the remote marine atmosphere. Marine aerosols are subject to losses due to precipitation, dry deposition, and coagulation; yet, observed remote marine aerosol concentrations and size distributions are relatively constant. This maintenance of the aerosol distribution requires a particle source. This work focuses on the potential of H_2SO_4 nucleation within the marine boundary layer (MBL) to supply these particles. Spatial and temporal variability in meteorology and species concentrations are considered in a mathematical model to evaluate the effect of natural deviations from average MBL conditions on the highly nonlinear aerosol system. A dynamic, vertically dimensioned, size-resolved aerosol model is used with parameterized heterogeneous chemical processes. The results suggest that MBL nucleation may be an important source of new particle number in the remote MBL. However, though our model shows that typical remote MBL aerosol distributions can on average be maintained by MBL nucleation and sea-salt emissions, large oscillations in particle number concentration occur. Because such oscillations are only occasionally reported in measurements, MBL nucleation may not be the dominant source of new particles in the remote MBL. The nucleation events, which cause these oscillations, are predicted to occur at the top of the MBL after rain and/or entrainment of clean free tropospheric air. Predictions are particularly sensitive to the H_2SO_4 accommodation coefficient, nucleation tuner, and washout efficiency. Reduction of the accommodation coefficient is shown to increase the predicted accumulation mode concentration because the nucleation rate is enhanced. Entrainment of clean free tropospheric air is shown to increase the frequency of nucleation events within the MBL and may help to explain the observed correlation between subsidence and MBL small particles. A small constant addition of particles from the free troposphere, ocean, etc. suppresses H_2SO_4 nucleation and can lead to a reduction in total predicted aerosol number. This is because nucleation events require low total aerosol surface area and the constant addition of particles reduces the severity of aerosol surface area minimums. Larger external aerosol sources can maintain the observed remote MBL aerosol distribution. However, the temporal and spatial variability of such sources could have a large impact on aerosol concentrations and requires further investigation.

1. Introduction

Marine aerosols affect the amount of solar energy absorbed by Earth by both directly reflecting sunlight and serving as cloud condensation nuclei (CCN) [*Coakley et al.*, 1983; *Fouquart and Isaka*, 1992]. Because CCN concentrations are low over the ocean compared to the continents, marine clouds have large droplets which are relatively inefficient at scattering light [*Pruppacher and Klett*, 1980]. Increases in the number of CCN cause the cloud droplets to become smaller and better at light scattering [*Twomey*, 1991]. In addition, the smaller drops are less likely to precipitate, thus potentially increasing the lifetime of the cloud [*Albrecht*, 1989]. Understanding both the natural production of marine CCN and the impact of continental and anthropogenic influences will help us to quantify the direct and indirect aerosol effects on global climate change.

The marine boundary layer (MBL) is the relatively well-mixed atmospheric layer above the ocean and below the thermal inversion coincident with the marine stratus cloud

Copyright 1999 by the American Geophysical Union.

Paper number 1998JD100080.
0148-0227/99/1998JD100080$09.00

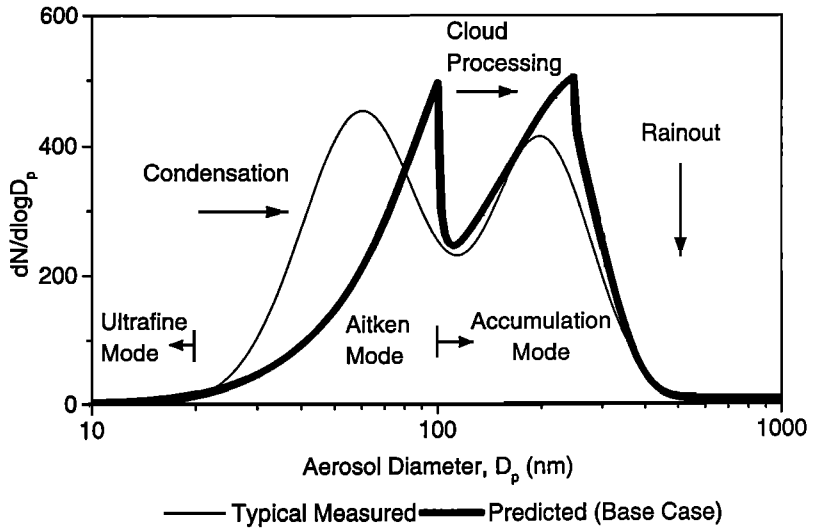

Figure 1. One hundred day average surface level aerosol predictions for the base case compared to a typical remote MBL aerosol number distribution based on the measurements of *Quinn et al.* [1996], *Clarke et al.* [1996], and *Van Dingenen et al.* [1995]. The dominant processes that lead to this bimodal distribution are also shown. The aerosol distribution is shown at a relative humidity of 80%.

deck. Aerosol number distributions in the MBL are characterized by a bimodal shape. Figure 1 shows a typical observed aerosol distribution based on measurements presented by *Van Dingenen et al.* [1995], *Quinn et al.* [1996], and *Clarke et al.* [1996]. Although the size and shape of these two modes vary, the general features are remarkably constant in remote MBL aerosol [*Fitzgerald,* 1991]. A typical number size distribution has an Aitken mode between 20 and 100 nm and an accumulation mode between 100 and 500 nm. The generally low concentration of ultrafine particles (less than 20 nm) is due to growth of MBL aerosol by condensation of gas-phase species, sulfuric acid (H_2SO_4), water, and ammonia in particular, and to a lesser extent by coagulation and low average nucleation rates. The sulfuric acid is generated by oxidation of dimethyl sulfide (DMS) [*Berresheim et al.*, 1995], which is emitted by phytoplankton from the ocean surface. Particles between 20 and 100 nm continue to grow by condensation but at slower rates because their surface area to volume ratio becomes increasingly smaller. The minimum between the Aitken and accumulation modes is generated by cloud processing [*Hoppel et al.*, 1990; 1994]. When particles large enough to act as CCN (greater than 100 nm) are activated into cloud droplets, sufficient liquid water is present to allow SO_2 to react rapidly with mainly hydrogen peroxide [*Russell et al.*, 1994]. As a result, sulfate mass is added to the cloud droplet. When the droplet evaporates, the aerosol that remains is larger than the original accumulation mode particle. Eventually, accumulation mode particles become large enough to precipitate out of the system.

These mechanisms for aerosol growth and removal have allowed estimates of MBL aerosol lifetime of less than 1 week [*Pandis et al.*, 1995; *Kerminen and Wexler*, 1997]. Yet, air commonly resides over the ocean in excess of 10 days and still maintains both the Aitken and accumulation modes [*Quinn et al.*, 1996]. This implies one or more sources of particles over the remote ocean to replenish losses due to precipitation, coagulation, and dry deposition.

Three hypotheses can be proposed to explain the necessary sources of new particles. The first is that new particles are directly emitted from the ocean. In particular the breaking of waves under windy conditions is known to produce aerosol particles. The second is that new particles are entrained from the free troposphere (FT) where they either were created by nucleation of gas-phase species at the lower temperatures of high altitudes or were transported from the continents. The third is that particles are created by nucleation of gas-phase species, such as sulfuric acid, within the MBL. High relative humidity (RH) in the MBL favors nucleation of H_2SO_4 with H_2O. Although each of these hypotheses is considered in this work, our primary focus will be on nucleation within the MBL.

1.1. Insights From Experimental Studies

Particles larger than 250 nm in dry diameter are primarily composed of sea salt, indicating direct emission from the ocean; particles less than 250 nm are primarily non-sea-salt sulfate, indicating the influence of H_2SO_4 and SO_2 gases on these aerosols [*Fitzgerald*, 1991; *Clarke et al.*, 1987; *Hoppel and Frick*, 1990; *Clarke and Porter*, 1993; *O'Dowd and Smith*, 1993; *Murphy et al.*, 1998]. In addition, a significant organic component has been seen [*Rivera-Carpio et al.*, 1996; *Gregory et al.*, 1996; *Murphy et al.*, 1998; *Middlebrook et al.*, 1998] mainly in particles smaller than 200 nm in diameter. Finally, measurements of trace metals and soot in remote marine aerosol samples indicate that in most cases transport of aerosol particles from continental regions is not a significant contributor [*Raemdonck et al.*, 1986].

Direct emission of aerosols from the ocean results from ocean whitecaps. *Monahan et al.* [1983] quantified the relationship between wind speed and the number and size of particles emitted. These particles are characterized by their sea-salt composition and tend to be greater than 100 nm in diameter. Indirect indications of smaller ocean derived particles are presented by *Clarke et al.* [1997] and direct

measurements are presented by *O'Dowd et al.* [1997] and *Murphy et al.* [1998].

Investigators have recently observed occasional instances in the MBL of ultrafine (3-20 nm) particles in large concentrations after rain and/or FT subsidence events [*Clarke et al.*, 1998; *Covert et al.*, 1992, 1996; *Weber et al.* 1995, 1998; *Hoppel et al.*, 1994]. These events may indicate MBL nucleation.

Raes et al. [1997] presented evidence of a FT source for MBL aerosol. Their conclusions were based on measurements in the MBL and FT at the same site and on back trajectory analysis. These measurements showed distinct similarities between the Aitken mode particles in the FT and MBL indicating that both air masses had the same FT particle source. In addition, *Covert et al.* [1996] and *Bates et al.* [1998] proposed that the FT is the source of Aitken mode particles based on observed dominance of the Aitken mode in areas of strong FT subsidence and entrainment.

1.2. Previous Theoretical Studies

Theoretical studies have also provided insights into the origin of new particles. Nucleation theory proposes that binary H_2SO_4 and H_2O nucleation proceeds at a highly nonlinear rate, which is a strong function of H_2SO_4 vapor concentration, temperature, and RH [*Jaeker-Voirol and Mirabel*, 1989]. This theory predicts H_2SO_4 threshold concentrations for nucleation to occur at given environmental conditions. MBL models [*Kerminen and Wexler*, 1995; *Raes et al.*, 1993; *Pandis et al.*, 1994, *Russell et al.*, 1994] show that the concentration of H_2SO_4 is controlled by the production of H_2SO_4 from SO_2 oxidation and the loss of H_2SO_4 is controlled by condensation onto existing particles. Because fresh nuclei are small (~3 nm), their creation does not significantly impact H_2SO_4 concentrations. Thus when the H_2SO_4 concentration exceeds the nucleation threshold value, new particles are created until either H_2SO_4 vapor production decreases or the new particles begin to contribute as a condensation sink for H_2SO_4, which may take several hours. The result is large bursts of new particle creation referred to as nucleation events.

Several modeling studies have attempted to determine the source of marine CCN. Most of these studies presumed that the thermal inversion between the MBL and FT is strong enough that the influence of the FT is negligible [*Lin et al.*, 1992; *Pandis et al.*, 1994; *Russell et al.*, 1994]. *Lin et al.* [1992] proposed that new particle formation occurs only when the preexisting aerosol number is very small. *Russell et al.* [1994] showed that MBL nucleation can generate sufficient new particles but only when rain events first clean the MBL of aerosol surface area. This allows H_2SO_4 to accumulate to levels high enough to allow nucleation events where several thousand new particles are created in a few hours. Dispersion could then supply these particles to adjacent air masses as a source of particles.

Raes [1995] and *Kerminen and Wexler* [1997] concluded that average remote MBL conditions both prevent nucleation and do not allow fresh nuclei to grow to become CCN within the relevant timescale. *Kerminen and Wexler* [1997] suggested that condensable vapors other than H_2SO_4 may be important. *Raes* [1995] proposed that DMS-derived H_2SO_4 in the FT can create the necessary small particles to maintain the observed MBL aerosol distribution. *Andrews et al.* [1997] addressed the potential of organics as nucleating and condensing species in the marine atmosphere. Their model assumed classic nucleation theory for the production of new organic particles. They concluded that measured ocean fluxes of organic vapors seem to be insufficient to account for the measured organic aerosol concentrations reported by *Rivera-Carpio et al.* [1996].

1.3. Remaining Questions

Despite the work of *Lin et al.* [1992], *Pandis et al.* [1994], and *Russell et al.* [1994] and in light of the competing evidence of *Raes* [1995] *and Kerminen and Wexler* [1997], it is unclear the extent to which nucleation in the MBL provides the particles necessary to maintain the MBL aerosol distribution. If we presume, as *Raes* [1995] and *Kerminen and Wexler* [1997] suggest, that typical remote MBL conditions do not allow maintenance of the aerosol size distribution, then what atypical conditions are required to create new particles in the MBL and do these conditions occur often enough to support the observed aerosol distribution?

1.4. Approach

A comprehensive approach is required, which includes detailed representations of time-dependent processes including aerosol nucleation, cloud processing, and precipitation. In particular, the highly nonlinear nature of the H_2SO_4 nucleation rate requires the consideration of nonaverage meteorological conditions. The effects of temporal variability in meteorological conditions can be addressed by randomizing discrete cloud and rain events. Spatial averaging may also be inappropriate if we consider the nonlinear effects of temperature and RH on nucleation rates [*Kerminen and Wexler*, 1995]. To account for these effects, temperature and RH vertical profiles will be resolved. In addition, cloud processing will be addressed in more detail because the rate at which accumulation mode particles grow to sizes large enough for precipitation removal impacts the frequency and magnitude of nucleation events. Finally, modeling of long simulation periods is necessary to both determine the interaction of meteorological events with dynamic species concentrations and to determine if H_2SO_4 nucleation can sustain MBL aerosol concentrations.

Individual aspects of this approach have been the focus of several previous investigations. In particular *Pandis et al.* [1994] and *Russell et al.* [1994] took a comprehensive long simulation time approach but were limited in the resolution of the aerosol spectrum. Spatial variability of temperature and RH were addressed by *Kerminen and Wexler* [1995], but cloud processing and precipitation were not. *Raes* [1995] focused on the interaction of the FT with the MBL over long periods and considered temporally resolved cloud and rain processes but did not include vertical resolution or sea salt. This work will address all of these issues in an integrated MBL model.

2. Model Description

A dynamic vertically resolved Lagrangian model based on the framework proposed by *Russell et al.* [1994] is used to predict the behavior of gas and aerosol species in the MBL. The lower boundary of the model is the ocean surface. The

upper boundary, at the thermal inversion above the marine stratus cloud deck, is set at 1 km. The space is discretized into ten equal vertical cells. Aerosol size is represented using 270 size sections evenly distributed in logarithmic space by diameter. The smallest size section is 3 nm, and the largest section is 5 μm. Modeled gas-phase species include DMS, SO_2, H_2SO_4, DMSO, OH, and NO_3.

The general differential equation for the change with time, t, of the ith aerosol size section or gas-phase species, C_i, is:

$$\frac{\partial C_i}{\partial t} = \frac{\partial}{\partial z}\left(K_{zz}\frac{\partial C_i}{\partial z}\right) + R_{gas}(C_j, \mathrm{OH}, \mathrm{NO}_3, T) + R_{cld}(C_j, i_{cld}) - R_{wdep}(C_i, i_{rain}) + R_{nuc}(C_{\mathrm{H_2SO_4}}, T, RH) + R_{coag}(C_j, RH) + R_{cnd}(C_{\mathrm{H_2SO_4}}, RH) \quad (1)$$

In this equation, K_{zz} is the turbulent diffusion constant for vertical transport; R_{gas} is the gas-phase chemical reaction rate; R_{cld} is the rate of aerosol growth or the gas-phase species concentration change due to aqueous-phase reactions in cloud droplets; R_{wdep} is the rate of species removal due to precipitation; and R_{nuc}, R_{coag}, and R_{cnd} are the rates of change of species i due to nucleation, coagulation, and condensation, respectively. Dependence on temperature, T, relative humidity, RH, species concentrations, C, and the existence of clouds, i_{cld}, or rain, i_{rain}, are indicated for each rate. This system of differential equations is subject to boundary conditions of

$$v_{entr} \cdot [C_{i,FT} - (C_i)_{z=H}] = K_{zz}\left(\frac{\partial C_i}{\partial z}\right)_{z=H} \quad (2)$$

at the top of the boundary layer, $z = H$, where v_{entr} is the entrainment velocity and $C_{i,FT}$ is the species concentration in the free troposphere, and

$$\left(v_{dry,i} \cdot C_i - K_{zz}\frac{\partial C_i}{\partial z}\right)_{z=0} = E_i - R_{ss} \quad (3)$$

at the surface, $z = 0$, where $v_{dry,i}$ is the deposition velocity of species i, E_i is ocean emission rate of species i, and R_{ss} is the rate of reaction with large sea-salt aerosols. The rate terms in equations (1)-(3) are discussed in detail in sections 2.2-2.11.

2.1. Vertical Transport

The vertical transfer rate of gases and aerosols is modeled according to K theory for turbulent mixing. This gradient driven approach uses a vertical transport constant, K_{zz}, of 20 $m^2\ s^{-1}$, which is estimated from the mesoscale meteorological model results of *Suhre and Rosset* [1994] and *Suhre et al.* [1995] for the MBL.

2.2. Gas-Phase Chemistry

The gas-phase chemical reaction rates for DMS oxidation, R_{gas}, are those used by *Pham et al.* [1995]. These reactions were determined to be adequate for predicting remote MBL sulfate concentrations [*Capaldo and Pandis*, 1997]. They include five reactions describing DMS oxidation by OH and NO_3, DMSO oxidation by OH, and SO_2 oxidation by OH to form H_2SO_4. The concentration of OH is assumed to follow sunlight intensity and is reduced by 50% during the occurrence of a cloud. The maximum OH concentration is 0.2 parts per trillion by volume (pptv). The NO_3 concentration is set to constant day and night values of 0 and 0.25 pptv respectively.

2.3. Cloud Processing

Cloud presence is stochastically determined every hour with a mean frequency of 0.3 per hour. The existence of a cloud is represented by the binary variable i_{cld} in equation (1). When a cloud exists, SO_2 is oxidized to sulfate in the top 100 m of the column and added to aerosols that are of sufficient size to activate as CCN (which corresponds to our accumulation mode, $D_p > 100$ nm at a reference RH of 80%). SO_2 is consumed assuming a first-order reaction with a rate constant of 2.4 h^{-1} based on the reactions presented by *Pandis and Seinfeld* [1989]. Gas-phase H_2SO_4 is completely transferred to the cloud droplet phase. The partitioning of the added sulfate onto the aerosol distribution is assumed to be proportional to the water uptake of the aerosol as it passes through the cloud. Using the model of *Gurciullo and Pandis* [1997], the average water volume, w_i (μm^3), of a CCN active aerosol in size section i passing through a remote MBL cloud can be parameterized as

$$w_i = \tfrac{\pi}{6}(9.7 \cdot D_{p,i}^{0.75})^3 \quad (4)$$

where D_p is in micrometers. The total cloud water concentration, w_T ($\mu m^3\ cm^{-3}$), is then

$$w_T = \sum_{CCN} w_i C_i \quad (5)$$

where the summation includes all CCN active aerosol size sections. The rate of sulfate volume increase of the ith section, $S_{cld,i}$ ($\mu m^3\ cm^{-3}\ h^{-1}$), can then be calculated as

$$S_{cld,i} = (2.4[\mathrm{SO_2}] + [\mathrm{H_2SO_4}])\frac{w_i C_i}{w_T}\frac{MW_{\mathrm{NH_4HSO_4}}}{\rho_{\mathrm{NH_4HSO_4}}}4.09\times10^{-5} \quad (6)$$

where $\rho_{NH_4HSO_4}$ is the density (g cm^{-3}) of dry ammonium bisulfate and the concentrations of SO_2 and H_2SO_4 are in pptv. The added sulfate causes the dry diameter to increase, but, because fixed aerosol size sections are used, the cloud processed particles are moved up to the appropriate size bins. The particles are distributed into the new size sections such that total number and mass (after the sulfate has been added) are conserved. $R_{cld,i}$ in equation (1) is calculated as the rate of concentration change of the ith section and includes both the addition of particles from smaller size sections and the removal of particles due to cloud processing growth.

The above size-dependent approach to cloud processing of SO_2 is in contrast to the uniform approach used in other models where the produced sulfate is evenly divided among all available accumulation mode particles [*Pandis et al.*, 1994; *Russell et al.*, 1994; *Raes*, 1995]. A comparison of these two approaches is presented in section 5.2.

2.4. Wet Deposition

Rain is also stochastically determined with an average frequency of one rain event every 2 days. Rain conditions are represented by the binary variable i_{rain} in equation (1). The wet removal rate, R_{wdep}, is parameterized independent of vertical position. To account for precipitation scavenging of gases and aerosols smaller than 250 nm, a Marshall-Palmer

raindrop size distribution for a rain intensity of 2 mm h^{-1} is used. This raindrop distribution results in a SO_2 scavenging rate of 0.67 h^{-1}. A coagulation model [*Seinfeld and Pandis*, 1998] is then used to determine the loss of aerosol particles due to falling rain drops under an assumed 98% RH. To represent in-cloud washout of particles, all aerosols with a diameter greater than 250 nm (at the reference RH of 80%) are removed.

Previous models [*Russell et al.*, 1994; *Raes*, 1995] assumed removal of a fixed fraction of all accumulation mode particles for a given rain event. Their approach is based on either the assumption that all cloud nucleating particles will produce cloud drops of about the same size or that cloud drop/raindrop collection efficiency is about the same over the cloud drop size distribution. However, for a marine cloud, larger cloud condensation nuclei become larger cloud droplets [*Flossmann*, 1991]. The largest of these will precipitate during a rain event because the collision efficiencies of large cloud droplets are dramatically greater than those less than 10 μm (the average size of a MBL cloud drop [*Seinfeld and Pandis*, 1998])[*Houghton*, 1985]. On the basis of this theory, the largest accumulation mode particles will be removed by precipitation. For simplicity, our model uses a critical washout diameter of 250 nm (at a reference RH of 80%) above which all particles are removed during a rain event. Although washout of all particles greater than 250 nm may be an unrealistic assumption, this parameterization does reproduce the surface area minima observed by *Clarke et al.* [1998]. A comparison of the fixed fraction versus critical washout diameter washout approaches is shown in section 5.1.

2.5. Nucleation

The nucleation rate, R_{nuc} (cm^{-3} h^{-1}), of H_2SO_4/H_2O is modeled according to *Jaeker-Voirol and Mirabel* [1989], with the addition of a nucleation tuner to account for observed discrepancies from nucleation theory in laboratory experiments. The parameterization of *Russell et al.* [1994] is expanded to include the dependence of the nucleation rate on temperature, T (Kelvin) [*Jaeker-Voirol and Mirabel*, 1989], as follows:

$$\log_{10}(R_{nuc}) = \log_{10}(k_n) - (64.24 + 4.7RH) + (6.13 + 1.95RH)\left(\log_{10}[H_2SO_4] + (298 - T)/25\right) \quad (7)$$

where RH is between zero and one and $[H_2SO_4]$ is in molecules per cm^3. Temperature and RH have prescribed linear profiles with altitude from 300 K and 80% RH at the surface to 290.5 K and 98% RH in the top vertical cell [*Susskind*, 1993].

In this work, a nucleation tuner, k_n, of 10^7 is used. This value is similar to that used by *Raes et al.* [1992] and *Russell et al.* [1994]. However, there is a large degree of uncertainty regarding the appropriate value of this parameter. *Kulmala et al.* [1998] describe a factor of 10^{-3} based on thermodynamic arguments. Experimental studies have indicated factors as low as 10^{-5} [*Wyslouzil et al.*, 1991]. Field studies have indicated that ammonia (NH_3) may participate in the creation of new nuclei [*Weber et al.*, 1998]. *Coffman and Hegg* [1995] apply a ternary nucleation theory for the $H_2SO_4/H_2O/NH_3$ system. Their results for an ammonia concentration of 1 pptv justify a H_2SO_4/H_2O nucleation tuner as high as 10^{10}. However, at H_2SO_4 concentrations of 0.4 pptv *Coffman and Hegg* [1995] show 7 orders of magnitude uncertainty due to disagreement in available thermodynamic parameters. In this work the nucleation tuner may be viewed as a correction factor for both the potential role of NH_3 and experimental uncertainties. The sensitivity of our model predictions to our choice of nucleation tuner will be quantified in section 5.4.

2.6. Coagulation

The coagulation rate of aerosol particles, R_{coag}, is modeled according to *Seinfeld and Pandis* [1998]. The diameter of the aerosol particle is adjusted to be in equilibrium with the ambient RH before the calculation. The dry aerosol diameter, $D_{p,dry}$, is increased to account for the addition of water vapor according to the following parameterization for ammonium bisulfate based on data presented by *Seinfeld and Pandis* [1998]

$$\frac{D_{p,wet}}{D_{p,dry}} = 17.8(RH - 50\%)^{3.5} + 1.28 \quad (8)$$

This equation is valid for RH between 50% and 98%. The mean aerosol size section wet diameter, $D_{p,wet}$, is calculated according to the above formula for the coagulation, condensation, and precipitation scavenging calculations. For the collection of interstitial aerosol by cloud droplets, an effective droplet diameter of 10 μm is assumed.

2.7. Condensation

The condensation rate of H_2SO_4, R_{cnd}, is calculated using the mass transfer model described by *Pandis et al.* [1994]. The accommodation coefficient, which accounts for interfacial mass transport limitations, is set at 0.2, which is the value reported by *Jefferson et al.* [1997] for H_2SO_4 condensation onto NaCl coated with low coverage of an organic, a composition supported by the measurements of *Murphy et al.* [1998]. Previous studies have used accommodation coefficients ranging from 0.02 to 1.0 [*Pandis et al.*, 1994; *Russell et al.*, 1994; *Kerminen and Wexler*, 1995, 1997; *Van Dingenen and Raes*, 1991; *Jefferson et al.*, 1997]. The sensitivity of the model to this parameter will be investigated in section 5.3.

2.8. Entrainment of FT Air

Free tropospheric air entrainment rates are modeled using an entrainment velocity, v_{entr}, of 0.5 cm s^{-1} [*Raes*, 1995] and the difference between the MBL and FT concentration of a given species (equation (2)). FT concentrations are kept constant during the simulation. Gas-phase species have zero free tropospheric concentrations except for SO_2 at 30 pptv. Aerosol measurements in the FT are scarce and show substantial variability with time and location [*Hudson et al.*, 1998; *Weber et al.*, 1995; *Raes et al.*, 1997; *Gregory et al.*, 1996; *Clarke et al.*, 1998]. For our base case, we assume that since turbulent mixing in the FT is much slower than in the MBL, the aerosol concentrations in the lower FT are similar to those of the MBL and the net aerosol exchange between the MBL and FT is negligible. However, since this may not be the case, we also explore the effects of assuming a FT aerosol distribution of 400 particles per cm^3 lognormally

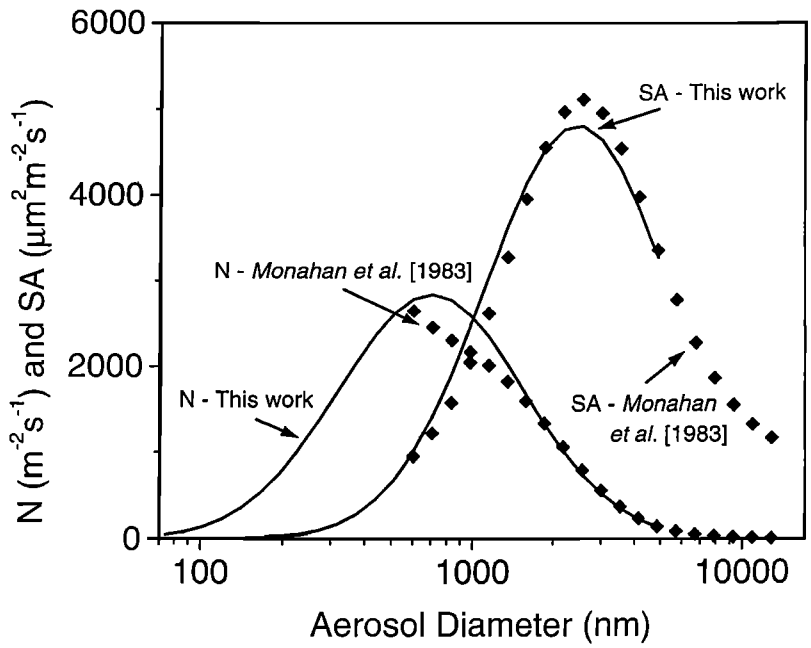

Figure 2. The sea-salt emissions used in this model (except for case 7) compared to those generated by the model of *Monahan et al.* [1983]. Number, *N*, and surface area, *SA*, are depicted.

distributed around 65 nm with a geometric standard deviation of 1.4 as predicted by *Raes* [1995]. In addition, we model an aerosol free FT and an intermediate case with 80 particles per cm^3.

2.9. Dry Deposition

Dry deposition rates are modeled using a species and aerosol size-dependent deposition velocity, $v_{dry,i}$ (equation (3)). Deposition velocities of 0.5 cm s^{-1} and 1.0 cm s^{-1} are used for SO_2 and H_2SO_4, respectively [*Voldner et al.*, 1986]. Aerosol dry deposition rates range from 0.1 to 0.015 cm s^{-1}, dependent on particle size according to *Hummelshoj et al.* [1992].

2.10. Emissions

The emission rate of species *i* from the ocean surface, E_i, applies for DMS at 5 μmol m^{-2} d^{-1} and sea-salt aerosol. The sea-salt emission is estimated according to *Monahan et al.* [1983] for a wind speed of 8 m s^{-1} to be about 3 cm^{-3} d^{-1} of accumulation mode particles. These are lognormally distributed with a mean of 700 nm and a geometric standard deviation of 2.2. The resulting number and surface area fluxes are compared in Figure 2 to the emissions fluxes generated by the model of *Monahan et al.* [1983]. Because sea-salt aerosols are important for maintaining MBL accumulation mode concentrations and provide the majority of the surface area upon which H_2SO_4 condenses, the sensitivity of our predictions to the sea-salt flux is addressed in section 5.5.

2.11. SO_2 Oxidation in Sea-Salt Particles

The oxidation rate of SO_2 in sea-salt particles, R_{SS} (equation (3)), is highly *p*H dependent and is modeled here as a function of the alkalinity flux [*Chameides and Stelson*, 1992]. The sulfate addition to sea-salt particles mainly occurs on a small number of large particles with relatively short lifetimes, and its direct contribution to aerosol growth can be neglected.

3. Results

A base case is presented to describe the dynamics of the MBL system when aerosol particles do not interact with the FT. This case describes a situation in which either the aerosol concentrations in the lower FT are approximately the same as those at the top of the MBL or where the entrainment of FT air is negligible. By eliminating the potential source of particles from the FT, we will be better able to examine the hypothesis that maintenance of the MBL aerosol distribution is controlled by MBL processes. Additional cases that address the incorporation of external sources including particle transfer from the FT will then be presented.

Simulations are for 100 days as to allow a large number of random occurrences of clouds and rain events to interact with various predicted aerosol distributions. The initial gas-phase concentrations are set to zero with the exception of the DMS concentration, which is set to 100 pptv. The initial aerosol size distribution is that of the typical measured MBL aerosol shown in Figure 1. In all figures presented in this work, aerosol diameters are reported assuming wet particles in thermodynamic equilibrium with a relative humidity of 80% according to equation (8).

4. Base Case: No Aerosol Interaction With FT

Figure 1 shows the 100 day average surface level aerosol distribution predicted for the base case conditions compared to the typical measured remote MBL aerosol. This long-term average reproduces the bimodal character of the MBL aerosol distribution. The accumulation mode matches well in both magnitude and mean diameter to the measured distribution.

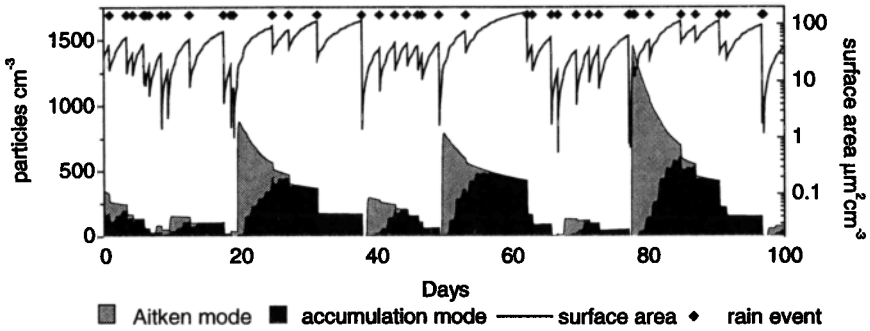

Figure 3. Time series of the surface level aerosol number concentration and surface area predicted for the base case in which there is no aerosol interaction between the MBL and FT. Rain events are shown as black dots. Grey and black sections show the partitioning of the predicted number between the Aitken mode (D_p < 100 nm at RH = 80%) and the accumulation mode (D_p > 100 nm at RH = 80%), respectively.

The Aitken mode is somewhat smaller and has a larger mean diameter than expected but seems to be within observed variability [*Quinn et al.*, 1996]. The sharp features of the predicted distribution at 100 and 250 nm are due to the invariant cutoffs of our model's representations of cloud processing and washout, respectively.

Figure 3 shows the predicted surface level aerosol number concentration for the simulation. The total number is subdivided into Aitken and accumulation mode particles based on a cutoff diameter of 100 nm. Rain events are indicated at the top of the figure. Aerosol surface area is also shown. Nucleation bursts occur every 7 to 19 days and produce distinct peaks in the Aitken mode. These events occur when aerosol surface area is low, which allows H_2SO_4 to accumulate above the threshold for nucleation. Reduction of aerosol surface area depends on the removal of large aerosol particles. This occurs most effectively through precipitation. Yet, rain events do not efficiently remove particles until they have grown through condensation up to accumulation mode size and then through repeated cloud processing cycles. In addition, nucleation event frequency is a function of the number of particles created. The larger the number of particles, the less sulfate is added per particle due to condensation and cloud processing. Therefore growth up to the washout diameter is slower.

Predicted gas-phase concentrations are consistent with observations from the remote MBL. DMS and SO_2 average predictions over all vertical cells are 114 and 30 pptv,

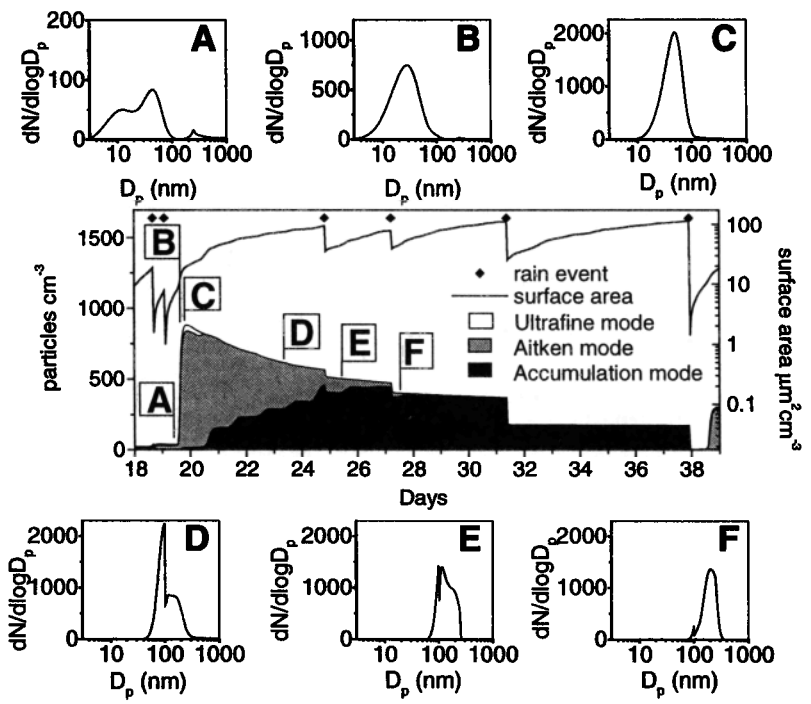

Figure 4. Predicted surface level aerosol concentration and surface area for the base case nucleation event on day 19. Cross sections, labeled A through F, show the aerosol size distribution at various times throughout the nucleation event. White, gray, and black sections show the partitioning of the predicted number between the ultrafine mode (3 nm < D_p < 20 nm at RH = 80%), Aitken mode (20 nm < D_p < 100 nm at RH = 80%), and the accumulation mode (D_p > 100 nm at RH = 80%), respectively.

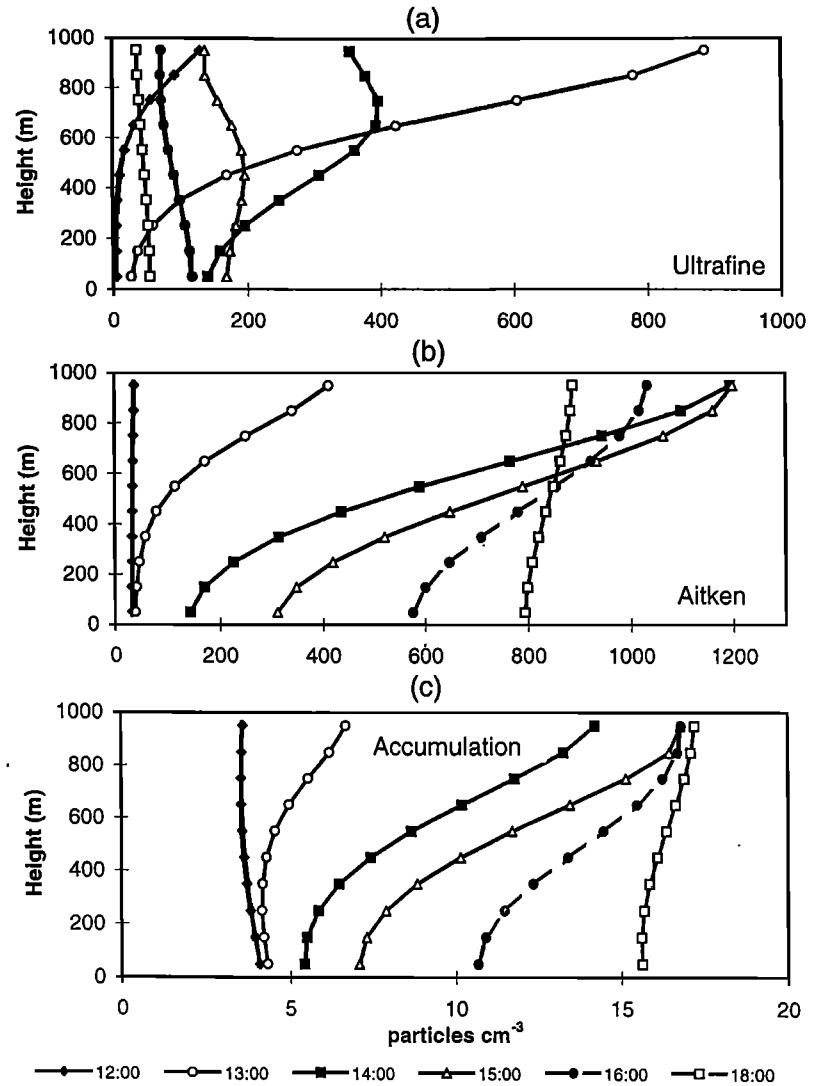

Figure 5. Vertical distribution of aerosol concentrations during the base case nucleation event on day 19. Predictions of (a) the ultrafine mode (3 nm < D_p < 20 nm at RH = 80%), (b) the Aitken mode (20 nm < D_p < 100 nm at RH = 80%), and (c) the accumulation mode (D_p > 100 nm at RH = 80%) are shown.

respectively. These are similar to the observations of *Gregory et al.* [1996], *Putaud et al.* [1993], *Bandy et al.* [1996], *Berresheim et al.* [1990], *Ayers et al.* [1995], and *Thornton and Bandy* [1993]. The predicted average H_2SO_4 concentration for the base case is 0.09 pptv with an average daily peak of 0.38 pptv. These are in agreement with the observations of *Weber et al.* [1995, 1997, 1998] and *Berresheim et al.* [1993].

Surface area predictions also match well with observations. This agreement occurs in both the average surface area of 50 μm^2 cm^{-3} [*Quinn et al.*, 1993; *Porter and Clarke*, 1997; *Jensen et al.*, 1996] and the minimum surface areas around 1 $\mu m^2 cm^{-3}$ [*Clarke et al.*, 1998].

4.1. Aerosol Dynamics During a Nucleation Event

Figure 4 depicts the aerosol distribution dynamics through the nucleation event on day 19. Concentrations are shown for the surface cell. At 1300 local time (LT) the aerosol concentration is low as a result of two rain events within the previous 24 hours. The H_2SO_4 concentration at this time is 0.8 pptv and the aerosol size distribution is shown in cross section A of Figure 4. At this time the nucleation event has begun at the top of the boundary layer (Figure 5a). The total number of particles at the surface is 44 per cm^3 with a surface area of 8.0 μm^2 cm^{-3}. By 1500 LT the nucleation event has produced surface level concentrations of about 400 new particles per cm^3 with a modal peak in diameter at 28 nm (Figure 4, cross section B). These freshly nucleated particles grow rapidly from their initial diameter of 3 nm because the H_2SO_4 concentration is high (1.4 pptv). Five hours later, the aerosol concentration (Figure 4, cross section C) has grown to 850 per cm^3 with a concentration peak at 47 nm. Fifteen particles per cm^3 exceed the accumulation mode critical diameter of 100 nm. At this point, because the sun has set, the OH concentration drops to zero, and no more H_2SO_4 is created. This "freezes" the growth of Aitken and ultrafine mode particles since they are not large enough to be processed by clouds. The day after the nucleation event, H_2SO_4 is once

again formed from SO_2 oxidation, but no significant nucleation occurs because the H_2SO_4 concentration (0.6 pptv daily maximum) is reduced by rapid condensation on the available aerosols. Although H_2SO_4 is added to all the particle sizes, the smallest particles grow faster because their surface area to mass ratio is the largest. The result is that the Aitken mode resumes growth but at a slower rate than the day of the nucleation event because the new accumulation mode particles act as a sink for most of the H_2SO_4 produced. The accumulation mode meanwhile continues to grow as a result of cloud processing. Four days after the nucleation event (Figure 4, cross section D), 291 particles per cm^3 are predicted in the accumulation mode, and a bimodal distribution is clearly seen. However, because there have been no new particles created, the Aitken mode has become narrow with a peak concentration at the cloud processing cutoff diameter of 100 nm. After 6 days (Figure 4, cross section E) the Aitken mode has all but disappeared. Until 12 days after the nucleation event, precipitation has been ineffective at removing aerosol because few particles have grown to sizes where washout is efficient. Figure 4, cross section F, shows the aerosol distribution following the rain event 8 days after nucleation (day 27). On day 31, a rain event removes roughly half of the accumulation mode number. Yet, it takes 19 days after the nucleation event (day 38) before accumulation mode growth due to cloud processing allows washout to remove a sufficient surface area for another nucleation event.

4.2. Vertical Profiles During a Nucleation Event

The vertical profiles of aerosol concentration during day 19 are shown in Figure 5. Ultrafine mode particles (3 nm < D_p < 20 nm), Aitken mode particles (20 nm < D_p < 100 nm) and accumulation mode particles (D_p > 100 nm) are shown in Figures 5a, 5b, and 5c, respectively. At 1200 LT, the nucleation event begins in the top cells. One hour later, the ultrafine mode shows about 900 particles per cm^3 in the top cell. The sharp vertical gradient is due to nucleation rates roughly 4 orders of magnitude greater in the top versus the bottom vertical cell. The difference in nucleation rates is caused by lower temperature and higher RH at the top of the MBL. Thus, nucleation occurs almost exclusively in the top vertical cell. The exception is when clouds are present and cloud droplets enhance the condensation rate of H_2SO_4. Under these conditions, nucleation often continues in the cell below the cloud layer, though at a reduced rate. On this day in particular, no clouds existed between the hours of 1000 and 1500 LT. Figures 5b and 5c show that within an hour of the nucleation event new particles have grown into the Aitken mode in concentrations exceeding 400 particles per cm^3 in the top cell and a couple particles per cm^3 have been added to the top cells of the accumulation mode. By 1400 LT vertical dispersion has transported 140 ultrafine particles per cm^3 to the surface and a peak in the ultrafine mode occurs at around 700 m. This peak is caused by coagulation of ultrafine and accumulation mode particles in the top cells where accumulation mode particles are in higher concentrations. Aitken mode particles peak in the top cell at 1200 particles per cm^3. Hours 1500 through 1800 LT show continued decline in ultrafine mode particles, vertical dispersion of Aitken particles down to the surface, and slow growth into the accumulation mode. It is important to note that within the first day of the nucleation event about 12 accumulation mode particles per cm^3 are created in the column.

4.3. Discussion of the Base Case

This production of accumulation mode particles within hours of a nucleation event appears to be in disagreement with the results of *Kerminen and Wexler* [1997], *Raes et al.* [1993], and *Raes* [1995]. These investigators suggest that nanometer sized particles cannot in a few days grow to accumulation mode particles by condensation of H_2SO_4 under the conditions of the MBL. The rapid growth of new particles in our model is dependent on a low total surface area available for H_2SO_4 condensation. The presence of accumulation mode particles in the model of *Kerminen and Wexler* [1997] greatly slows new particle growth. Thus it is in the dynamics of the system that a reasonable mechanism for nuclei growth appears, and models that rely on average conditions may not be able to capture the features important to understanding the system.

The conclusion of *Kerminen and Wexler* [1995] that nucleation occurs at the top of the MBL is supported by both our model (Figure 5) and the observations of *Clarke et al.* [1998]. In addition, our model shows that aerosol nucleation and the subsequent growth of new particles takes place within timescales that are comparable to the vertical mixing rate of the MBL (see Figure 5). Because nucleation and cloud processing occur at the top of the MBL and measurements are often taken at the surface, consideration of the vertical structure of the MBL is important.

Figures 3 and 4 demonstrate that the number of Aitken and accumulation mode particles varies from a few particles per cm^3 to hundreds or even thousands of particles per cm^3. This is consistent with observed accumulation mode concentrations. Measurements reported by *Raes et al.* [1997] and *Hegg et al.* [1991] indicate brief absences of the accumulation mode, and, since our model only predicts concentrations less than 10 particles per cm^3 for short periods, the predicted accumulation mode oscillations are not a weakness of this simulation. On the contrary, although Aitken mode particles are occasionally reported both below 10 particles per cm^3 and above 600 particles per cm^3 [*Quinn et al.*, 1996], our base case simulation predicts much lower and higher Aitken mode concentrations for time periods spanning days. This indicates that MBL nucleation, as described in this simulation, is not likely to be the main source of particle number in the remote MBL, despite the model's ability to reasonably reproduce accumulation mode concentrations. This suggests either that a source of small particles may be absent from our base case scenario or that particles are grown too rapidly into the accumulation mode. We will discuss further these possibilities in the following sections.

5. Sensitivity to Modeling Parameterizations

5.1. Washout

Instead of removing all particles greater than 250 nm during a precipitation event, case 2 employs a washout parameterization in which a constant fraction of all accumulation mode particles are removed. This is the approach used in the zero dimensional models of *Russell et*

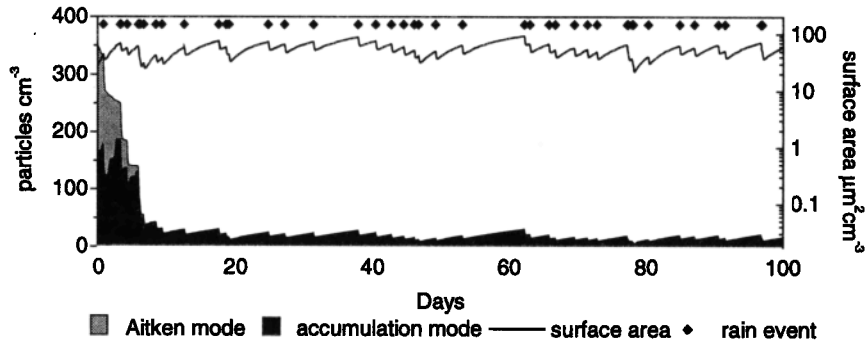

Figure 6. Time series of surface level aerosol number concentration and surface area predicted for case 2 in which an accumulation mode size independent washout parameterization is used. Rain events are shown as black dots. Grey and black sections show the partitioning of the predicted number between the Aitken mode (D_p < 100 nm at RH = 80%) and the accumulation mode (D_p > 100 nm at RH = 80%), respectively.

al. [1994] and *Raes* [1995]. Figure 6 shows the 100 day time series aerosol predictions when all accumulation mode particles in the cloud containing fraction of the MBL are removed from the system during precipitation. Recall that when a cloud is present in our model all accumulation mode particles become cloud droplets in the top 100 m of the MBL. During rain events, turbulent dispersion supplies additional particles to the cloud, which are then removed as well through washout. Both this approach and the base case on average remove similar number and surface area of particles. However, case 2 does so by removing a similar fraction of accumulation mode particles for each rain event (~20%), whereas the base case removes very few particles when accumulation mode particles are small and most of the accumulation mode when these particles are large. The effect is that in the base case sharp minima of surface area allow large nucleation events (Figure 3). In case 2, more gradual changes in surface area produce no significant nucleation (Figure 6). As a result predicted concentrations in case 2 are low, on average 33 particles per cm^3, despite a similar average surface area (54 μm^2 cm^{-3}) to the base case (Table 1 and Figure 6). These two cases demonstrate that the model predictions are very sensitive to the washout parameterization and that continued investigations of aerosol removal in the MBL are necessary.

5.2. Sulfate Allocation During Cloud Processing

The effect of aerosol size independent production of sulfate from cloud processing of SO_2 is examined in case 3. This approach results in faster growth of small accumulation mode particles since the same quantity of sulfate is added to both small and large particles. The differences in the average aerosol concentrations compared to the base case (Table 1) are due to more rapid growth of accumulation mode particles up to the washout diameter. This reduces the average accumulation mode concentration by 17% and allows larger nucleation events, which result in a 61% larger Aitken mode prediction.

5.3. Accommodation Coefficient for H_2SO_4

Cases 4 and 5 show the sensitivity of the predictions to the accommodation coefficient for condensation of H_2SO_4.

Table 1. Summary of 100 Day Average Surface Level Predictions

Simulation	Ultrafine, cm^{-3}	Aitken, cm^{-3}	Accum, cm^{-3}	Surface Area, μm^2 cm^{-3}	Particles Added Over Base Case, cm^{-3} d^{-1}
Typical measured aerosol (see text)	*	180	170	27	---
Base case: No aerosol interaction with FT	2	119	194	50	---
Alternate Process Parameterizations					
Case 2: Size independent washout	0	5	27	54	---
Case 3: Size independent cloud processing	3	191	161	53	---
Case 4: H_2SO_4 accommodation coefficient of 0.1	11	189	197	50	---
Case 5: H_2SO_4 accommodation coefficient of 0.4	0	34	125	40	---
Case 6: Nucleation tuner of 10^6	1	64	133	43	---
Case 7: Doubled sea-salt emissions	1	94	184	65	---
Case 8: Constant RH (90%) and temperature (295 K) with height	5	153	164	46	---
MBL-Free Troposphere Interaction					
Case 9: No aerosols in FT	4	119	58	24	-78
Case 10: 80 cm^{-3} in FT (mean D_p = 65 nm, STD = 1.4)	1	46	55	23	-10
Case 11: 400 cm^{-3} in FT (mean D_p = 65 nm, STD = 1.4)	0	175	151	34	32
Case 12: Daily random entrainment (0.2 d^{-1}), 80 cm^{-3} in FT (see text)	2	67	72	28	-26
Case 13: Nucleation tuner of 10^{10}, 150 cm^{-3} in FT (mean D_p = 65 nm, STD = 1.4), and 0.2 d^{-1} entrainment	46	287	152	38	---
Added Constant Sources (No FT Interaction)					
Case 14: Nucleation source at D_p = 3 nm	53	109	120	42	240
Case 15: Ocean source of 11.4 μg m^{-2} d^{-1} (mean D_p = 60 nm, STD = 1.5)	0	131	220	54	48

*A typical UFCN concentration is not presented owing to the limited number of observations in this size range.

Average ultrafine, Aitken, and accumulation mode concentrations are predicted to increase with a decrease in the accommodation coefficient (Table 1). This can be explained in the following way. Decreasing the accommodation coefficient results in slower transfer of H_2SO_4 to the particle. This slows particle growth but also generates higher H_2SO_4 vapor concentrations, which lead to larger nucleation burst. Increasing the number of available nuclei leads to higher concentrations of all particle sizes. In cases 4 and 5 the nucleation driven effect dominates. The result is increases in predictions of all three modes with reductions in the accommodation coefficient. This trend has also been observed by *Russell et al.* [1994], *Pandis et al.* [1994], and *Kerminen and Wexler* [1995].

5.4. Nucleation Tuner

Case 6 shows the sensitivity of our predictions to decreasing the nucleation tuner. As seen in Table 1, decreasing the instantaneous nucleation rate by a factor of 10 reduces the ultrafine, Aitken, and accumulation mode concentrations by factors of 2, 1.9, and 1.5, respectively. Since nucleation is the only source of ultrafine and Aitken mode particles in this case, the response of these two modes is less than what might be expected. This result can be explained by two factors. First, a lower nucleation rate results in lower coagulation losses during and after nucleation events. Second, a negative feedback results from condensation of H_2SO_4 on the newly formed particles. This feedback allows the H_2SO_4 concentration to remain above the nucleation event threshold for longer periods if the nucleation rate is smaller because the surface area of the new particles does not become significant as quickly. The result is longer nucleation events for smaller nucleation tuner values.

The sensitivity of the system to a factor of 10 increase in the nucleation tuner was also calculated (results not shown) and the same trends are observed. Similar responses of the MBL system to a more comprehensive series of nucleation tuner and accumulation coefficient values are presented by *Russell et al.* [1994].

5.5. Sea-salt Emissions

Surface area affects the competition between H_2SO_4 nucleation and condensation, and sea-salt emissions are a major source of aerosol surface area in the MBL. To investigate the role of the sea salt, case 7 shows the effect of doubling the number of particles (and surface area) emitted as sea salt. Results show a 30% increase in the average predicted surface area (Table 1). The frequency of nucleation bursts is decreased compared to the base case leading to a 21% decrease in the average Aitken mode predictions and a 5% decrease in the average accumulation mode (Figure 7). The lesser effect on the accumulation mode is due to the increased sea-salt emissions in this range. The relative insensitivity of predictions to sea-salt emissions shown by case 7 may be surprising considering the sensitivity of the H_2SO_4 concentration to increases in surface area and the much larger sensitivity of the nucleation rate to the H_2SO_4 concentration. This is the result of the timing of the nucleation events that occur after sharp decreases in the surface area caused by rain. Thus, although the average surface area is sensitive to sea-salt emissions, the minima of the surface area following rain events, which control the nucleation burst magnitude, are somewhat less sensitive (Figure 7).

5.6. Vertical Resolution of Temperature and Relative Humidity

To evaluate the effect of the vertical temperature and RH resolution used in the base case, we assume constant temperature (295 K) and RH (90%) for all heights (case 8). Average surface level predictions are higher by 150% and 29% for ultrafine and Aitken modes, respectively, and lower by 15% for the accumulation mode compared to the base case (Table 1). These increases in ultrafine and Aitken mode concentrations are rather unexpected since equation (7) indicates a decrease in the total nucleation rate (given constant H_2SO_4 concentration) due to lowering the RH and raising the temperature in the top of the MBL. However, because aerosol size increases with increasing RH (equation (8)), condensation of H_2SO_4 is accelerated under high RH. For the base case, the top of the MBL (290 K, 98% RH), where almost all of the nucleation is predicted to occur, has higher nucleation rates because of the temperature and RH effects on equation (7) but lower H_2SO_4 concentrations, due to the RH effect on condensation. Case 8 both alters this competition and distributes the nucleation events to all vertical cells. The distribution of nucleation events minimizes losses due to coagulation of ultrafine particles. The net result is a relatively small change in overall Aitken and

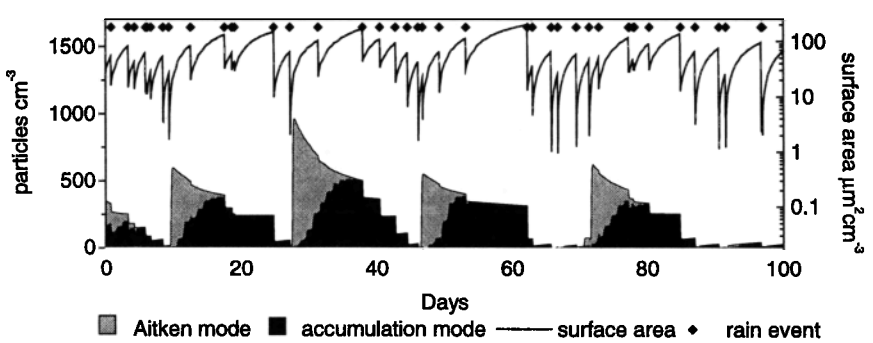

Figure 7. Time series of surface level aerosol number concentration and surface area predicted for case 7 in which the sea-salt emissions flux is doubled. Rain events are shown as black dots. Grey and black sections show the partitioning of the predicted number between the Aitken mode (D_p < 100 nm at RH = 80%) and the accumulation mode (D_p > 100 nm at RH = 80%), respectively.

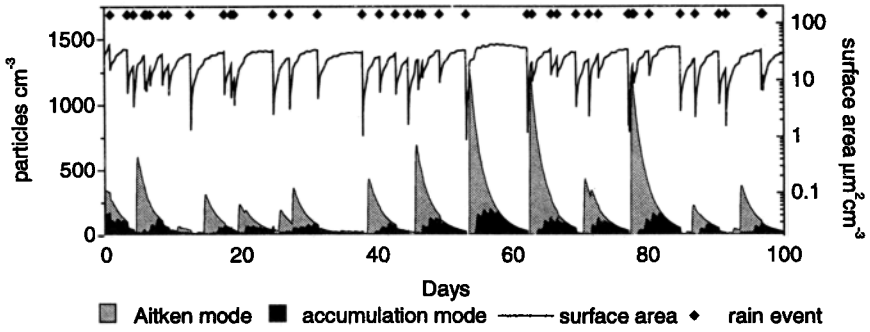

Figure 8. Time series of surface level aerosol number concentration and surface area predicted for case 9 in which the MBL interacts with a particle free FT. Rain events are shown as black dots. Grey and black sections show the partitioning of the predicted number between the Aitken mode (D_p < 100 nm at RH = 80%) and the accumulation mode (D_p > 100 nm at RH = 80%), respectively.

accumulation mode predictions despite large changes in the rates of the various processes.

6. MBL-Free Troposphere Interactions

Cases 9-13 are scenarios where Aitken mode particles in the FT serve to moderate MBL Aitken mode oscillations by diluting high concentrations and providing a source when concentrations are low. This interaction may be particularly important considering the inability of the base case to maintain measured Aitken mode concentrations between nucleation events. These FT particles could be the result of nucleation of H_2SO_4 in the upper FT as suggested by *Raes et al.* [1993]. Because FT aerosol measurements are variable and FT mixing is slow, the FT aerosols in this work are distributed according to the "self-preserving" aerosol distribution described by *Friedlander* [1977] with a mean diameter of 65 nm and a standard deviation of 1.4 [*Raes*, 1995].

6.1. FT Dilution

Figure 8 shows predictions for the theoretically limiting case where the MBL aerosol is diluted by entrainment of FT air that is completely free of aerosol particles. Entrainment of clean FT air produces two results. First, the average concentrations of aerosol particles of all sizes are reduced because of dilution at an average rate of 51 particles cm^{-3} d^{-1} for Aitken mode and 25 particles cm^{-3} d^{-1} for accumulation mode particles (based on an entrainment velocity of 0.5 cm s^{-1} and a 1000 m mixing height). Second, there is a 50% increase in the frequency of nucleation events over the base case because aerosol surface area is lost as accumulation mode concentrations are reduced by dilution. The magnitudes of nucleation events are similar to the base case. The effects of increases in both nucleation rates and accumulation mode loss are seen in Figure 8 and Table 1 as a 100% increase in ultrafine particles, the same average Aitken mode prediction, and a 70% decrease in accumulation mode concentrations compared to the base case. As in the base case, the Aitken mode is lost half way between nucleation events. Finally, since FT dilution significantly reduces aerosol surface area, rain events play a less important role in preceding nucleation. Evidence of the importance of FT entrainment in accumulation mode concentrations is seen in the relatively smooth decrease in the accumulation mode following nucleation events (Figure 8). This is in contrast to the accumulation mode step reductions in the base case, which are caused by rain.

In studies by *Raes et al.* [1993] and *Raes* [1995] entrainment has been associated with a positive flux of particles from the FT. This has in part been owing to an observed correlation between regions of FT subsidence and ultrafine or Aitken mode aerosol concentrations [*Bates et al.*, 1998; *Covert et al.*, 1996]. The results of case 9 suggest an alternative explanation for this correlation. If particle free air enters the system, then nucleation within the MBL can be enhanced leading to increases in ultrafine aerosol number.

6.2. Eighty Particles per cm^3 in the FT

Figure 9 shows the predicted time series of particle number concentration at the surface for a more realistic "clean" case where FT air contains 80 particles per cm^3 (mean D_p = 65 nm, STD = 1.4)(case 10). This time series shows that nucleation event frequency is increased over the base case due to dilution of large particles as in case 9. Yet, nucleation event frequency is reduced compared to case 9. Compared to both the base case and case 9, nucleation event magnitude is reduced. This is because when Aitken mode concentrations in the MBL become low, Aitken mode particles from the FT are transported into the MBL and provide a source of aerosol surface area sufficient to reduce gas-phase H_2SO_4 concentrations. This can either keep H_2SO_4 concentrations below the threshold for a nucleation event or reduce the severity of a threshold exceedance, which decreases the magnitude of the nucleation event. Although the FT source of Aitken mode particles is insufficient to support the observed MBL aerosol concentration (Table 1), the Aitken mode is maintained above 18 particles per cm^3 between nucleation events. Finally, both the reduction in the number of new particles generated through nucleation and the dilution of high MBL Aitken and accumulation mode concentrations due to entrainment reduces the average total aerosol prediction by 68% over the base case and 43% over case 9 (Table 1).

6.3. Four Hundred Particles per cm^3 in the FT

Case 11 considers a constant FT aerosol concentration of 400 particles per cm^3 (mean D_p = 65 nm, STD = 1.4). This

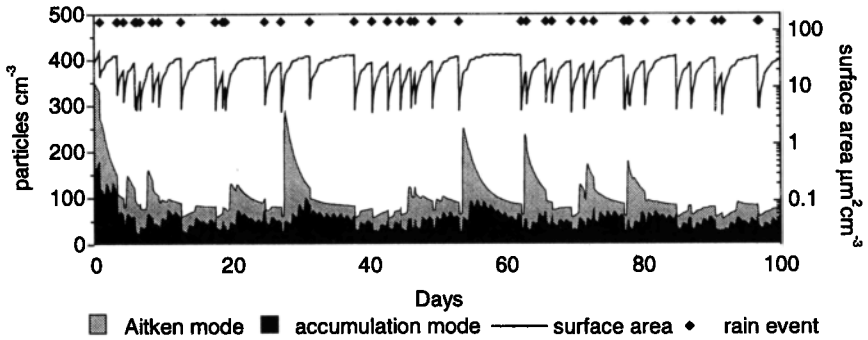

Figure 9. Time series of surface level aerosol number concentration and surface area predicted for case 10 where the MBL interacts with a FT containing a constant distribution of 80 particles per cm^3 distributed around a mean diameter of 65 nm with a standard deviation of 1.4. Rain events are shown as black dots. Grey and black sections show the partitioning of the predicted number between the Aitken mode (D_p < 100 nm at RH = 80%) and the accumulation mode (D_p > 100 nm at RH = 80%), respectively.

concentration is similar to that used by *Raes* [1995] and is supported by the measurements presented by *Russell et al.* [1998]. This scenario provides roughly 97 particles cm^{-3} d^{-1} to the Aitken mode from the FT. The net particle flux from the FT is 32 cm^{-3} d^{-1} (Table 1) because of dilution of accumulation mode particles. The model predicts that this continuous particle source is sufficient to support the observed aerosol distribution in the remote MBL without any nucleation events (Figure 10). Thus, despite washout and FT dilution of accumulation mode particles, the surface area provided to the MBL by a constant supply of FT Aitken mode particles is sufficient to keep H_2SO_4 concentrations below the nucleation event threshold.

6.4. Variable Entrainment

In cases 9-11, constant entrainment is considered with a velocity of 0.5 cm s^{-1}. For case 12, the same net entrainment is produced, but entrainment is randomly determined every day with a frequency of 0.2 d^{-1}, such that on days when entrainment occurs a velocity of 2.5 cm s^{-1} is used. This stochastic entrainment scheme is applied with FT aerosol concentrations of 80 particles per cm^3 as in case 10. As can be seen in Figure 11 and Table 1, there is an increase in both the Aitken mode predictions by 46% and the accumulation mode by 31% over case 10. However, these concentrations still only account for 40% of the typical measured aerosol. It should be noted that this random scheme is somewhat arbitrary, although entrainment velocities of even greater magnitude are estimated by *Russell et al.* [1998]. In addition, variability in FT aerosol concentration could be high, especially considering the slow mixing rates (K_{zz} < 1 m^2 s^{-1}, *Suhre et al.*, [1995]) in the FT and the potential of wind direction decoupling between the lower FT and the MBL. FT aerosol concentrations have been observed to range from around 200 particles per cm^3 to several thousand particles per cm^3 [*Russell et al.*, 1998; *Clarke et al.*, 1998; *Raes et al.*, 1997]. In addition to case 12, simulations were also performed with a daily random entrainment frequency of 0.5 d^{-1} and hourly random entrainment frequencies of 0.5 h^{-1} and 0.2 h^{-1}. For all of these cases, average predictions were similar to the constant entrainment case 10. This indicates that the system is relatively insensitive to time variable entrainment rates.

6.5. Increased Nucleation With FT Entrainment

Case 13 considers the use of a nucleation tuner of 10^{10}, 150 particles per cm^3 in the FT, and a random daily entrainment of 0.2 d^{-1}. The resulting predictions are seen in Figure 12 and

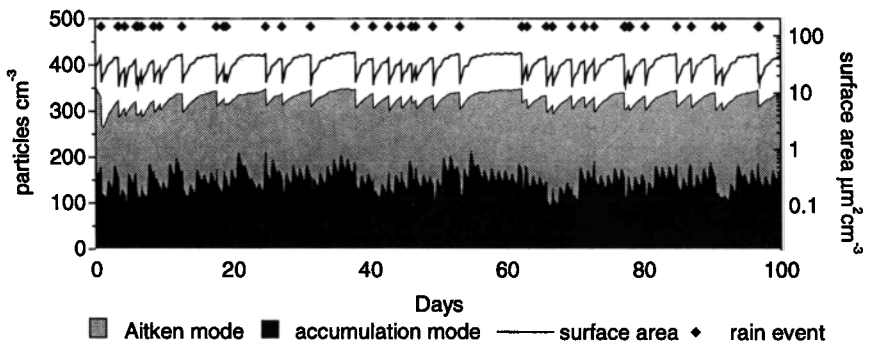

Figure 10. Time series of surface level aerosol number concentration and surface area predicted for case 11 where the MBL interacts with a FT containing a constant distribution of 400 particles per cm^3 distributed around a mean diameter of 65 nm with a standard deviation of 1.4. Rain events are shown as black dots. Grey and black sections show the partitioning of the predicted number between the Aitken mode (D_p < 100 nm at RH = 80%) and the accumulation mode (D_p > 100 nm at RH = 80%), respectively.

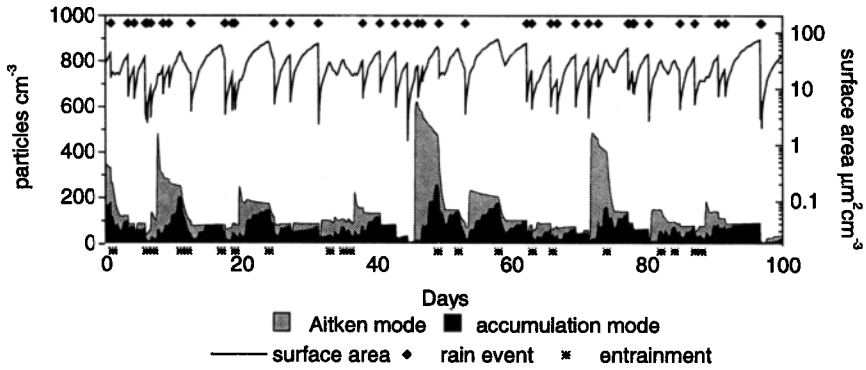

Figure 11. Time series of surface level aerosol number concentration and surface area predicted for case 12 where the MBL interacts with a FT using randomly occurring entrainment (v_{entr} = 2.5 cm s^{-1}, frequency = 0.2 d^{-1}) where entrainment occurs only on days designated with an asterisk. The FT contains a constant 80 particles per cm^3 (mean D_p = 65 nm, STD = 1.4 at RH = 80%). Rain events are shown as black dots. Grey and black sections show the partitioning of the predicted number between the Aitken mode (D_p < 100 nm at RH = 80%) and the accumulation mode (D_p > 100 nm at RH = 80%), respectively.

Table 1. With this combination of parameters, our model predicts MBL aerosol concentrations in general agreement with observations. Of note is the generally consistent presence of the Aitken mode, although high concentrations are still common. Also, Table 1 shows an average ultrafine concentration of 46 particles per cm^3. This high average concentration of ultrafine particles is supported by the observations of *Bates et al.* [1998].

7. Additional Constant Aerosol Sources

The response of the system is examined for both an additional constant nucleation source and an ocean source of Aitken mode particles. Case 14 presents a modification to the nucleation rate that differs functionally from the nucleation tuner. The nucleation tuner is the common means of accounting for unknown nucleation sources, but it assumes the same functional form as that of binary H_2SO_4/H_2O nucleation theory. Case 14 presents a constant additional nucleation source of 240 particles cm^{-3} d^{-1} at 3 nm in addition to the nucleation rate equation used in the base case. As is seen in Table 1, this is a sufficient particle source to maintain typical measured remote MBL aerosol concentrations. As in case 11, no nucleation bursts occur. This constant nucleation source is characterized by continuous existence of ultrafine particles, including a peak at 3 nm. Note however that such a persistent ultrafine aerosol concentration has not been observed.

Case 15 simulates the behavior of the MBL when an additional ocean source of small particles is constantly supplied. Specifically, 11.4 μg m^{-2} d^{-1} distributed with a mean diameter of 60 nm and a standard deviation of 1.5 are supplied to generate a source of 48 particles cm^{-3} d^{-1}. This source could represent Aitken mode sea-salt emissions as supported by measurements presented by *O'Dowd et al.* [1997] and *Murphy et al.* [1998] or organic aerosol emission as suggested by *Andrews et al.* [1997]. As in cases 11 and 14, this source is sufficient to maintain the typical remote MBL aerosol distribution without nucleation bursts (Table 1). Note that this is 5 times fewer added particles than case 14. This

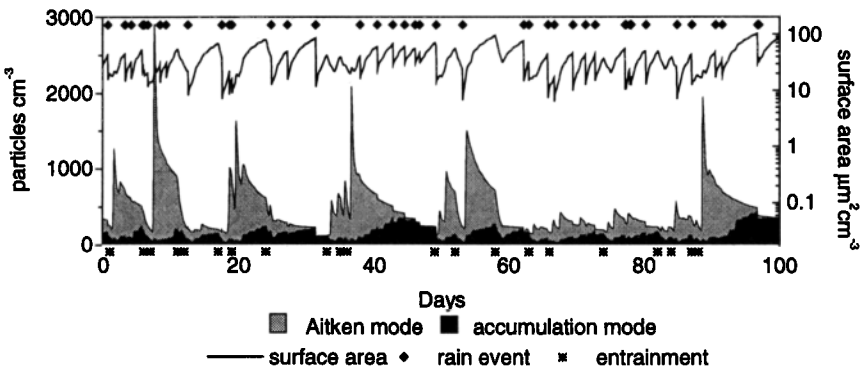

Figure 12. Time series of surface level aerosol number concentration and surface area predicted for case 13 in which a nucleation tuner of 10^{10} is used, the FT contains a constant 150 particles per cm^3 (mean D_p = 65 nm, STD = 1.4 at RH = 80%), and the MBL interacts with a FT using randomly occurring entrainment (v_{entr} = 2.5 cm s^{-1}, frequency = 0.2 d^{-1}). Entrainment occurs only on days designated with an asterisk. Rain events are shown as black dots. Grey and black sections show the partitioning of the predicted number between the Aitken mode (D_p < 100 nm at RH = 80%) and the accumulation mode (D_p > 100 nm at RH = 80%), respectively.

difference is primarily a result of coagulation of ultrafine particles in case 14. Although cases 14 and 15 do not have strong theoretical justifications for the new particle distributions used, they do demonstrate the type and magnitude of sources that can maintain the MBL aerosol distribution independent of free tropospheric interaction.

8. Discussion and Conclusions

This work shows that consideration of a MBL source of particles from H_2SO_4 nucleation is important in developing our understanding of the aerosol distribution in the remote MBL. With only H_2SO_4 nucleation and sea-salt emissions, the MBL can theoretically maintain a reasonable average aerosol number and size distribution despite losses due to precipitation, coagulation, dry deposition, and dilution due to FT entrainment. Nucleation is predicted to occur in bursts creating 100 to 2000 particles per cm^3 with a frequency of one event per 5-20 days. These events occur after rain or entrainment of clean FT air reduces aerosol surface area in the MBL. Nucleation is predicted to occur at the top of the MBL where temperature is low and humidity is high. Predicted accumulation mode (D_p > 100 nm) concentrations are generally consistent with observations. However, Aitken mode particles (20 nm < D_p < 100 nm) are predicted to oscillate between lows and highs that are generally outside the range of observations. To maintain reasonable Aitken mode particle concentrations an additional and more constant source seems to be necessary. This source is most likely from the free troposphere [*Raes et al.*, 1997; *Bates et al.*, 1998; *Andronache, et al.*, 1997] but could also be due to horizontal diffusion within the MBL or from an unaccounted for ocean source. Yet, including such a source limits nucleation and may suggest that increased nucleation rates as high as 10^{10} times that of classical binary nucleation theory for the H_2SO_4/H_2O system [*Jaeker-Voirol and Mirabel*, 1989] are required.

The key to understanding the character of H_2SO_4 nucleation is the highly nonlinear nature of this particle source. Nucleation occurs when the H_2SO_4 concentration exceeds a threshold value determined by the temperature and RH of the air parcel. Accumulation of H_2SO_4 only occurs when losses due to condensation onto aerosol particles are limited by low aerosol surface area. Reduction of aerosol surface area is a necessary precursor to nucleation and occurs when rain removes large particles and/or clean air is entrained into the MBL. Vertical resolution and stochastic cloud and rain events allow more accurate prediction of the environmental conditions that lead to MBL nucleation than the average meteorological conditions used in previous models.

Because nucleation occurs under conditions of low surface area and high H_2SO_4 concentration, the first several hours of a nucleation event allow for rapid growth of the new particles. This can generate a small number of accumulation mode particles within a few hours of a nucleation event. Later, growth is slowed by reduction in H_2SO_4 concentration due to the newly created aerosol surface area.

After particles enter the system (through nucleation, emission, or transport) their growth is dominated by condensation of H_2SO_4 and oxidation of SO_2 in cloud droplets. Modeling of the condensation process is dependent on the choice of accommodation coefficient. Reducing the accommodation coefficient is shown to increase both Aitken mode and accumulation mode concentrations by shifting the competition between H_2SO_4 nucleation and condensation toward nucleation.

Adding size-dependent partitioning of sulfate produced by SO_2 oxidation in cloud droplets affects the loss rate of accumulation mode particles. When compared to a size-independent processing scheme similar to those used by *Russell et al.* [1994] and *Raes* [1995], the parameterization presented in this model predicted slower accumulation mode growth up to the critical washout diameter, which resulted in a 20% increase in accumulation mode particles. However, this tended to maintain enough aerosol surface area to reduce nucleation rates leading to a 38% reduction in Aitken mode predictions.

The model results were found to be sensitive to the washout parameterization. An accumulation mode particle size independent washout rate [*Russell et al.*, 1994; *Raes*, 1995] was compared to a critical diameter washout scheme (base case). Although both parameterizations remove similar fractions of both accumulation mode number and surface area, the base case predicts 7 times the accumulation mode particles and 24 times the Aitken mode concentration despite similar predicted average surface area. This difference is due to the variance in surface area removed during particular rain events. The sensitivity of the system to rain parameterization warrants future investigation into this area. In particular, the simple modeling schemes presented here do not include any dependence between accumulation mode concentrations and cloud activation diameter, rain characteristics, or cloud microphysics.

Interaction with the free troposphere can increase the frequency of nucleation events by dilution of MBL aerosols, and it can provide a source of Aitken mode particles to the system when aerosol concentrations are low. However, addition of particles to the system, whether from the FT or from some other source, suppresses nucleation because the increased surface area from the external particles lowers the H_2SO_4 concentration. Reasonable external sources, in particular the FT aerosol distribution of *Raes* [1995], can maintain the observed MBL aerosol distribution; however, such a flux of particles completely suppresses MBL nucleation. Addition of anthropogenic aerosol would be expected to suppress nucleation in a similar way.

Direct enhancement of the binary H_2SO_4/H_2O nucleation rate determined by classical theory (through use of a nucleation tuner) appears to be necessary in order to predict ultrafine and Aitken mode oscillations as they have been observed in the remote MBL [*Bates et al.*, 1998; *Clarke et al.*, 1998; *Covert et al.*, 1992, 1996; *Weber et al.*, 1995, 1998; *Hoppel et al.*, 1994]. A nucleation tuner between 10^7 and 10^{10} can adequately describe MBL aerosol behavior in our model. Support for such a large deviation from classical theory for binary H_2SO_4/H_2O nucleation [*Jaeker-Voirol and Mirabel*, 1989] may involve interaction of the nuclei with as little as 1 pptv of ammonia [*Coffman and Hegg*, 1995]. The use of such a large tuner, however, points to the necessity of further study in this area.

Because both MBL nucleation and input of external sources can generate the observed remote MBL aerosol concentrations, multiple particle sources may maintain MBL

aerosol concentrations. The frequency with which each of the sources described here may supply particles to the system depends upon the temporal and spatial dynamics of these external sources. The system is relatively insensitive to time variable entrainment, though it should be noted that no correlations between clouds or precipitation and entrainment were included in our model. In addition, this work does not address variable FT aerosol concentrations, changes in the height of the MBL, the presence of convective clouds, zonal subsidence patterns, or horizontal diffusion. All such processes could impact aerosol predictions especially given the threshold-like nature of nucleation events.

Although our results suggest that the MBL aerosol distribution can on average be maintained in both number and modal character by H_2SO_4 nucleation and sea-salt emissions within the MBL, observational support for the predicted oscillatory nature of this system is only occasionally reported [*Clarke et al.*, 1998; *Covert et al.*, 1992, 1996; *Weber et al.*, 1995, 1998; *Hoppel et al.*, 1994]. The predicted oscillations in the Aitken mode and the sensitivity of the nucleation rate to external sources suggest that consideration of the MBL as a horizontally homogeneous unit interacting with a constant FT is insufficient for determining the natural source of particles over the remote ocean.

Acknowledgment. This work was supported by the National Science Foundation under agreement ATM-9508051.

References

Albrecht, B. A., Aerosols, cloud microphysics, and fractional cloudiness, *Science*, *245*, 1227-1230, 1989.

Andrews, E., S. M. Kreidenweis, J. E. Penner, and S. M. Larson, Potential origin of organic cloud condensation nuclei observed at marine site, *J. Geophys. Res.*, *102*, 21,997-22,012, 1997.

Andronache, C., W. L. Chameides, D. D. Davis, B. E. Anderson, R. F. Pueschel, A. R. Bandy, D. C. Thornton, R. W. Talbot, P. Kasibhatla, and C. S. Kiang, Gas-to-particle conversion of tropospheric sulfur as estimated from observations in the western North Pacific during PEM-West B, *J. Geophys. Res.*, *102*, 28,511-28,538, 1997.

Ayers, G. P., S. T. Bentley, J. P. Ivey, and B. W. Forgan, Dimethylsulfide in marine air at Cape Grim, 41°S, *J. Geophys. Res.*, *100*, 21,013-21,021, 1995.

Bandy, A. R., D. C. Thornton, B. W. Blomquist, S. Chen, T. P. Wade, J. C. Ianni, G. M. Mitchell, and W. Nadler, Chemistry of dimethyl sulfide in the equatorial Pacific atmosphere, *Geophys. Res. Lett.*, *23*, 741-744, 1996.

Bates, T. S., V. N. Kapustin, P. K. Quinn, D. S. Covert, D. J. Coffman, C. Mari, P. A. Durkee, W. J. De Bruyn, and E. S. Saltzman, Processes controlling the distribution of aerosol particles in the lower marine boundary layer during the First Aerosol Characterization Experiment (ACE 1), *J. Geophys. Res.*, *103*, 16,369-16,383, 1998.

Berresheim, H., M. O. Andreae, G. P. Ayers, R. W. Gillett, J. T. Merrill, V. J. Davis, and W. L. Chameides, Airborne measurements of dimethylsulfide, sulfur dioxide, and aerosol ions over the Southern Ocean south of Australia, *J. Atoms. Chem.*, *10*, 341-370, 1990.

Berresheim, H., F. L. Eisele, D. J. Tanner, L. M. McInnes, D. C. Ramsey-Bell, and D. S. Covert, Atmospheric sulfur chemistry and cloud condensation nuclei (CCN) concentrations over the northeastern Pacific coast, *J. Geophys. Res.*, *98*, 12,701-12,711, 1993.

Berresheim, H., P. H. Wine, and D. D. Davis, Sulfur in the atmosphere, in *Composition, Chemistry, and Climate of the Atmosphere*, edited by H. B. Singh, chap. 8, pp. 251-307, Van Nostrand Reinhold, New York, 1995.

Capaldo, K. P., and S. N. Pandis, Dimethylsulfide chemistry in the remote marine atmosphere: Evaluation and sensitivity analysis of available mechanisms. *J. Geophys. Res.*, *102*, 23,251-23,267, 1997.

Chameides, W. L., and A. W. Stelson, Aqueous-phase chemical processes in deliquescent sea-salt aerosols: A mechanism that couples the atmospheric cycles of S and sea salt, *J. Geophys. Res.*, *97*, 20,565-20,580, 1992.

Clarke, A. D., and J. N. Porter, Pacific marine aerosol, 2, Equatorial gradients in chlorophyll, ammonium, and excess sulfate during SAGA 3, *J. Geophys. Res.*, *98*, 16,997-17,010, 1993.

Clarke, A. D., N. C. Ahlquist, and D. S. Covert, The Pacific marine aerosol: Evidence for natural acid sulfates, *J. Geophys. Res.*, *92*, 4179-4190, 1987.

Clarke, A. D., Z. Li, and M. Litchy, Aerosol dynamics in the equatorial Pacific marine boundary layer: Microphysics, diurnal cycles, and entrainment, *Geophys. Res. Lett.*, *23*, 733-736, 1996.

Clarke, A. D., T. Uehara, and J. N. Porter, Atmospheric nuclei and related aerosol fields over the Atlantic: Clean subsiding air and continental pollution during ASTEX, *J. Geophys. Res.*, *102*, 25,281-25,292, 1997.

Clarke, A. D., J. L. Varner, F. Eisele, R. L. Mauldin, D. Tanner, and M. Litchy, Particle production in the remote marine atmosphere: Cloud outflow and subsidence during ACE 1, *J. Geophys. Res.*, 103, 16,397-16,409, 1998.

Coakley, J. A., Jr., R. D. Cess, and F. B. Yurevich, The effect of tropospheric aerosols on the Earth's radiation budget: A parameterization for climate models, *J. Atmos. Sci.*, *40*, 116-138, 1983.

Coffman, D. J., and D. A. Hegg, A preliminary study of the effect of ammonia on particle nucleation in the marine boundary layer, *J. Geophys. Res.*, *100*, 7147-7160, 1995.

Covert, D. S., V. N. Kapustin, P. K. Quinn, and T. S. Bates, New particle formation in the marine boundary layer, *J. Geophys. Res.*, *97*, 20,581-20,589, 1992.

Covert, D. S., V. N. Kapustin, T. S. Bates, and P. K. Quinn, Physical properties of marine boundary layer aerosol particles of the mid-Pacific in relation to sources and meteorological transport, *J. Geophys. Res.*, *101*, 6919-6930, 1996.

Fitzgerald, J. W., Marine aerosols: A review, *Atmos. Environ., Part A*, *25A*, 533-545, 1991.

Flossmann, A. I., The scavenging of two different types of marine aerosol particles calculated using a two-dimensional detailed cloud model, *Tellus, Ser. B*, *43B*, 301-321, 1991.

Fouquart, Y., and H. Isaka, Sulfur emission, CCN, clouds and climate: A review, *Ann. Geophys.*, *10*, 462-471, 1992.

Friedlander, S. K., *Smoke, Dust and Haze: Fundamentals of Aerosol Behavior*, John Wiley, New York, 1977.

Gregory, G. L., A. S. Bachmeier, D. R. Blake, B. G. Heikes, D. C. Thornton, A. R. Bandy, J. D. Bradshaw, and Y. Kondo, Chemical signatures of aged Pacific marine air: Mixed layer and free troposphere as measured during PEM-West A, *J. Geophys. Res.*, *101*, 1727-1742, 1996.

Gurciullo, C. S. and S. N. Pandis, Effect of composition variations in cloud droplet populations on aqueous-phase chemistry. *J. Geophys. Res.*, *102*, 9375-9385, 1997.

Hegg, D. A., L. F. Radke, and P. V. Hobbs, Measurements of Aitken nuclei and cloud condensation nuclei in the marine atmosphere and their relation to the DMS-cloud-climate hypothesis, *J. Geophys. Res.*, *96*, 18,727-18,733, 1991.

Hoppel, W. A. and G. M. Frick, Submicron aerosol size distributions measured over the tropical and south Pacific, *Atmos. Environ., Part A*, *24A*, 645-659, 1990.

Hoppel, W. A., J. W. Fitzgerald, G. M. Frick, and R. E. Larson, Aerosol size distribution and optical properties found in the marine boundary layer of the Atlantic Ocean, *J. Geophys. Res.*, *95*, 3659-3686, 1990.

Hoppel, W. A., G. M. Frick, J. W. Fitzgerald, and R. E. Larson, Marine boundary layer measurements of new particle formation and the effects which nonprecipitating clouds have on the aerosol size distribution, *J. Geophys. Res.*, *99*, 14,443-14,459, 1994.

Houghton, H. G., *Physical Meteorology*, MIT Press, Cambridge, Mass., 1985.

Hudson, J. G., Y. Xie, and S. S. Yum, Vertical distributions of cloud condensation nuclei spectra over the summertime Southern Ocean, *J. Geophys. Res.*, *103*, 16,609-16,624, 1998.

Hummelshoj, P., N. O. Jensen, and S. E. Larsen, Particle dry deposition to a sea surface, in *Precipitation Scavenging and*

Atmosphere Surface Exchange, edited by S. E. Schwartz, and W. G. N. Slinn, pp. 829-840, Hemishere Pub. Co., Washington, 1992.

Jaeker-Voirol, A., and P. Mirabel, Heteromolecular nucleation in the sulfuric acid-water system, *Atmos. Environ.*, *23*, 2053-2057, 1989.

Jefferson, A., F. L. Eisele, P. J. Ziemann, R. J. Weber, J. J. Marti, and P. H. McMurry, Measurements of the H_2SO_4 mass accommodation coefficient onto polydisperse aerosol, *J. Geophys. Res.*, *102*, 19,021-19,028, 1997.

Jensen, T. L., S. M. Kreidenweis, Y. Kim, H. Sievering, and A. Pszenny, Aerosol distributions in the North Atlantic marine boundary layer during the Atlantic Stratocumulus Transition Experiment/Marine Aerosol and Gas Exchange, *J. Geophys. Res.*, *101*, 4455-4497, 1996.

Kerminen, V.-M., and A. S. Wexler, Enhanced formation and development of sulfate particles due to marine boundary layer circulation, *J. Geophys. Res.*, *100*, 23,051-23,062, 1995.

Kerminen, V.-M., and A. S. Wexler, Growth behavior of the marine submicron boundary layer aerosol. *J. Geophys. Res.*, *102*, 18,813-18,825, 1997.

Kulmala, M., A. Laaksonen, and L. Pirjola, Parameterizations for sulfuric acid/water nucleation rates, *J. Geophys. Res.*, *103*, 8301-8307, 1998.

Lin, X., W. L. Chameides, C. S. Kiang, A. W. Stelson, and H. Berresheim, A model study of the formation of cloud condensation nuclei in remote marine areas, *J. Geophys. Res.*, *97*, 18,161-18,171, 1992.

Middlebrook, A. M., D. M. Murphy, and D. S. Thomson, Observations of organic material in individual particles at Cape Grim during the First Aerosol Characterization Experiment (ACE 1), *J. Geophys. Res.*, *103*, 16,475-16,483, 1998.

Monahan, E. C., C. W. Fairall, K. L. Davidson, and P. J. Boyle, Observed inter-relations between 10 m winds, ocean whitecaps and marine aerosols, *Q. J. R. Meteorol. Soc.*, *109*, 379-392, 1983.

Murphy, D. M., J. R. Anderson, P. K. Quinn, L. M. McInnes, F. J. Brechtel, S. M. Kreidenweis, A. M. Middlebrook, M. Posfai, D. S. Thomson, and P. R. Buseck, Influence of sea-salt on aerosol radiative properties in the Southern Ocean marine boundary layer, *Nature*, *392*, 62-65, 1998.

O'Dowd, C. D., and M. H. Smith, Physicochemical properties of aerosols over the northeast Atlantic: Evidence for wind-speed-related submicron sea-salt aerosol production, *J. Geophys. Res.*, *98*, 1137-1149, 1993.

O'Dowd, C. D., M. H. Smith, I. E. Consterdine, and J. A. Lowe, Marine aerosol, sea-salt, and the marine sulphur cycle: A short review, *Atmos. Environ.*, *31*, 73-80, 1997.

Pandis, S. N., and J. H. Seinfeld, Sensitivity analysis of a chemical mechanism for aqueous-phase atmospheric chemistry, *J. Geophys. Res.*, *94*, 1105-1126, 1989.

Pandis, S. N., L. M. Russell, and J. H. Seinfeld, The relationship between DMS flux and CCN concentration in remote marine regions, *J. Geophys. Res.*, *99*, 16,945-16,957, 1994.

Pandis, S. N., A. S. Wexler, and J. H. Seinfeld, Dynamics of tropospheric aerosols. *J. Phys. Chem.*, *99*, 9646-9659, 1995.

Pham, M., J.-F. Muller, G. P. Brasseur, C. Granier, and G. Megie, A three-dimensional study of the tropospheric sulfur cycle, *J. Geophys. Res.*, *100*, 26,061-26,092, 1995.

Porter, J. N., and A. D. Clarke, Aerosol size distribution models based on in situ measurements, *J. Geophys. Res.*, *102*, 6035-6045, 1997.

Pruppacher, H. R., and J. C. Klett, *Microphysics of Clouds and Precipitation*, D. Reidel, Norwell, Mass., 1980.

Putaud, J. P., S. Belviso, B. C. Nguyen, and N. Mihalopoulos, Dimethylsulfide, aerosols, and condensation nuclei over the tropical northeastern Atlantic Ocean, *J. Geophys. Res.*, *98*, 14,863-14,871, 1993.

Quinn, P. K., D. S. Covert, T. S. Bates, V. N. Kapustin, D. C. Ramsey-Bell, and L. M. McInnes, Dimethylsulfide/cloud condensation nuclei/climate system: Relevant size-resolved measurements of the chemical and physical properties of atmospheric aerosol particles, *J. Geophys. Res.*, *98*, 10,411-10,427, 1993.

Quinn, P. K., V. N. Kapustin, T. S. Bates, and D. S. Covert, Chemical and optical properties of marine boundary layer aerosol particles of the mid-Pacific in relation to sources and meteorological transport, *J. Geophys. Res.*, *101*, 6931-6951, 1996.

Raemdonck, H., W. Maenhaut, and M. O. Andreae, Chemistry of marine aerosol over the tropical and equatorial Pacific, *J. Geophys. Res.*, *91*, 8623-8636, 1986.

Raes, F., Entrainment of free tropospheric aerosols as a regulating mechanism for cloud condensation nuclei in the remote marine boundary layer, *J. Geophys. Res.*, *100*, 2893-2903, 1995.

Raes, F., A. Saltelli, and R. Van Dingenen, Modeling formation and growth of H_2SO_4-H_2O aerosols-Uncertainty analysis and experimental evaluation, *J. Aerosol Sci.*, *23*, 759-771, 1992.

Raes, F., R. Van Dingenen, J. Wilson, and A. Saltelli, Cloud condensation nuclei from dimethylsulphide in the natural marine boundary layer: Remote vs. in-situ production, in *Dimethylsulphide: Oceans, Atmosphere, and Climate*, edited by G. Restelli and B. Angeletti, pp. 311-322, Kluwer Acad., Norwell, Mass. 1993.

Raes, F., R. Van Dingenen, E. Cuevas, P. F. J. Van Velthoven, and J. M. Prospero, Observations of aerosols in the free troposphere and marine boundary layer of the subtropical northeast Atlantic: Discussion of processes determining their size distribution, *J. Geophys. Res.*, *102*, 21,315-21,328, 1997.

Rivera-Carpio, C. A., C. E. Corrigan, T. Novakov, J. E. Penner, C. F. Rodgers, and J. C. Chow, Derivation of contributions of sulfate and carbonaceous aerosols to cloud condensation nuclei from mass size distributions, *J. Geophys. Res.*, *101*, 19,483-19,493, 1996.

Russell, L. M., S. N. Pandis, and J. H. Seinfeld, Aerosol production and growth in the marine boundary layer, *J. Geophys. Res.*, *99*, 20,989-21,003, 1994.

Russell, L. M., D. H. Lenschow, K. K. Laursen, P. B. Krummel, S. T. Siems, A. R. Bandy, D. C. Thornton, and T. S. Bates, Bidirectional mixing in an ACE 1 marine boundary layer overlain by a second turbulent layer, *J. Geophys. Res.*, *103*, 16,411-16,432, 1998.

Seinfeld, J. H., and S. N. Pandis, *Atmospheric Chemistry and Physics from Air Pollution to Climate Change*, John Wiley, New York, 1998.

Suhre, K., and R. Rosset, DMS oxidation and turbulent transport in the marine boundary layer: A numerical study, *J. Atmos. Chem.*, *18*, 379-395, 1994.

Suhre, K., M. O. Andreae, and R. Rosset, Biogenic sulfur emissions and aerosols over the tropical South Atlantic, 2, One-dimensional simulation of sulfur chemistry in the marine boundary layer, *J. Geophys. Res.*, *100*, 11,323-11,334, 1995.

Susskind, J., Water vapor and temperature, in *Atlas of satellite observations related to global climate change*, edited by R. J. Gurney, J. L. Foster, and C. L. Parkinson, pp. 89-128, Cambridge Univ. Press, New York, 1993.

Thornton, D. C., and A. R. Bandy, Sulfur dioxide and dimethyl sulfide in the central Pacific troposphere, *J. Atmos. Chem.*, *17*, 1-13, 1993.

Twomey, S. A., Aerosols, clouds, and radiation, *Atmos. Environ., Part A*, *25A*, 2435-2442, 1991.

Van Dingenen, R., and F. Raes, Determination of the condensation accommodation coefficient of sulfuric acid on water-sulfuric acid aerosol, *Aerosol Sci. Technol.*, *15*, 93-106, 1991.

Van Dingenen, R., F. Raes, and N. R. Jensen, Evidence for anthropogenic impact on number concentration and sulfate content of cloud processed aerosol particles over the north Atlantic, *J. Geophys. Res.*, *100*, 21,057-21,067, 1995.

Voldner, E. C., L. A. Barrie, and A. Sirois, A literature review of dry deposition of oxides of sulfur and nitrogen with emphasis on long-range transport modelling in North America, *Atmos. Environ.*, *20*, 2101-2123, 1986.

Weber, R. J., P. H. McMurry, F. L. Eisele, and D. J. Tanner, Measurement of expected nucleation precursor species and 3 to 500 nm diameter particles at Mauna Loa Observatory, Hawaii, *J. Atmos. Sci.*, *52*, 2242-2257, 1995.

Weber, R. J., J. J. Marti, P. H. McMurry, F. L. Eisele, D. J. Tanner, and A. Jefferson, Measurements of new particle formation and ultrafine particle growth rates at a clean continental site, *J. Geophys. Res.*, *102*, 4375-4385, 1997.

Weber, R. J., P. H. McMurry, L. Mauldin, D. J. Tanner, F. L. Eisele, F. J. Brechtel, S. M. Kreidenweis, G. L. Kok, R. D. Schillawski, and D. Baumgardner, A study of new particle formation and growth involving biogenic and trace gas species measured during ACE 1, *J. Geophys. Res.*, *103*, 16,385-16,396, 1998.

Wyslouzil, B. E., J. H. Seinfeld, R. C. Flagan, and K. Okuyama, Binary nucleation in acid-water systems, II, Sulfuric acid-water and comparison with methanesulfonic acid-water, *J. Chem. Phys.*, *10*, 6842-6850, 1991.

K.P. Capaldo and S.N. Pandis, Department of Chemical Engineering, Carnegie Mellon University, Pittsburgh, PA 15213. (e-mail: spyros@andrew.cmu.edu)

P. Kasibhatla, Nicholas School of the Environment, Duke University, Durham, NC 27708.

(Received March 17, 1998; revised November 10, 1998; accepted November 13, 1998.)